JOURNAL OF MATERIALS SCIENCE 25 (1990) 207–214

Evaluation by indentation of fracture toughness of ceramic materials

K. M. LIANG
Tsinghua University, Beijing, People's Republic of China
G. ORANGE, G. FANTOZZI
GEMPPM, INSA de Lyon, 69621 Villeurbanne, France

A transition fracture mode from Palmqvist to median has been observed in a number of ceramic materials. A new expression to determine the fracture toughness (K_{IC}) by indentation is presented. The K_{IC} values calculated by this formula are independent of the crack profile (median or Palmqvist) and of the applied load. This formula has been obtained by modifying the universal curve of Evans and Charles to incorporate Palmqvist and median cracks over a wide range of loads in the case of brittle materials with different mechanical properties (elastic properties: E, ν, K_{IC}).

1. Introduction

The fracture toughness, or the critical stress intensity factor (K_{IC}), can be considered as one of the most important fracture properties of structural ceramic materials. The conventional ways to determine K_{IC} (by single edge notched beam (SENB), chevron notched beam (CVNB) and double cantilever beam (DCB)) require complex experimental procedure and a minimum number of samples which have quite large dimensions. Recently, there have been several attempts to use the indentation method which could be considered as a simpler technique to obtain the fracture toughness values of brittle materials [1–3]. This technique requires only a small polished area on the specimen surface from which a large number of data points can be generated rapidly.

In principle, indentation methods require measurement of the size of the cracks formed around the indent at loads in excess of the critical load, P_0, which is required to initiate the cracks (around the indent). After measuring the indentation parameters (e.g. the indentation radius, the crack length and the applied load), we can use one of several expressions (listed in Table I) which have been developed by different authors to obtain K_{IC} values.

However, there are specific conditions and limitations for using these formulae because some of them are related to the treatment of indentation data on the basis of a median crack (Fig. 1a) and the others on the basis of a Palmqvist crack (Fig. 1b); moreover some of these are restricted to certain materials. Up to now, no universal formula has been available to evaluate real values of K_{IC} using any crack profile produced over a large range of loads for all ceramic materials.

The aim of this paper is to observe the characteristics of crack profiles from Palmqvist type to median type in the case of different materials, or at different loads for the same material, and to find out the relationship of fracture data to the ratio c/a (c is the crack length and a is the half diagonal length of the indent (Fig. 1a)) and to the elastic properties of materials (elastic modulus, Poisson's ratio).

We have performed indentation experiments using both low (1 to 50 N) and high (100 to 500 N) loads for zirconia-toughened alumina dispersoid composites. A new formula which yields acceptable values of K_{IC} over the entire range of loads has been put forward, taking into consideration the role of Poisson's ratio.

2. Literature review

Surface cracks associated with Vickers indentation are now widely used to estimate fracture toughness of ceramics and cermets. Crack profiles induced by indentation may be classified into two types: median type and Palmqvist type.

2.1. Crack of median type

A fundamental study of the median crack problem, based on Griffith–Irwin fracture mechanics, has recently been developed [11]. Lawn and Fuller [12], working primarily on glasses, discovered that the crack radius c increased with load P as

$$c = kP^{2/3} \quad (1)$$

where k is an empirically derived constant. Marshall and Lawn [13], on the basis of experimental observations, changed the form of Equation 1 and obtained

$$K_C = \chi P/c^{2/3} \quad (2)$$

for well-developed indentation cracks (Fig. 1a), where K_C is the toughness of the indented material and χ is a constant to be determined for any given indentation/specimen system.

During recent years many studies of indentation fracture in ceramic materials have been performed. Evans and Charles [1], according to the relationship of

0022–2461/90 $03.00 + .12

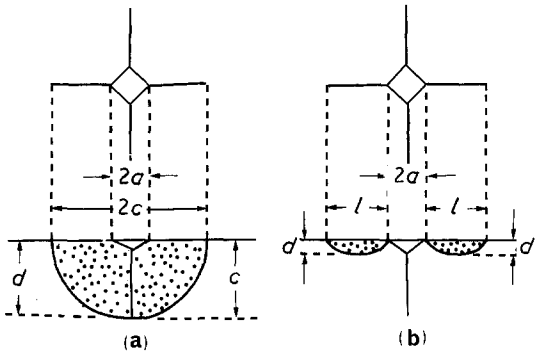

Figure 1 Comparison of (a) median and (b) Palmqvist cracks around a Vickers indentation.

hardness and diagonal of indent

$$H = P/\alpha_0 a^2 \quad (3)$$

changed the form of Equation 2 into

$$\frac{K_C \phi}{Ha^{1/2}} = g(c/a)^{-3/2} \quad (4)$$

where $g = 0.48$, ϕ is a constraint factor (≈ 3) and H is the hardness of the indented material.

Niihara *et al.* [4], working on hot-pressed SiC, hot-pressed Si_3N_4 and B_4C, sintered SiC, chemical vapour-deposited Si_3N_4 and soda–lime–silica glasses, found a value of g close to 0.203 (Formula A).

Using Equation 2 or 4, Evans and Charles [1] discovered that there is no exact coincidence of the fracture data ($K_C\phi/Ha^{1/2}$) for the different materials tested in their study. Evans and Charles [1], Lawn *et al.* [6] and Anstis *et al.* [5] analysed this problem. From the analysis of elastic–plastic field, they considered that the volume of plastic zone is accommodated by the surrounding elastic matrix. In this way, the constant χ depends on the ratio of Young's modulus to hardness, E/H, to a power m:

$$\chi = \beta_1 (E/H)^m \quad (5)$$

where β_1 is a material-independent constant for Vickers-produced radial cracks. Evans and Charles [1] obtained $m = 0.4$; Lawn *et al.* [6] and Anstis *et al.* [5] obtained $m = 0.5$. Following the approach of Lawn *et al.* [6], Laugier [9] obtained an analysis approximation $m = 2/3$.

With $m = 0.4$, Blendell [14] obtained a new expression

$$\left(\frac{K_{IC}\phi}{Ha^{1/2}}\right)\left(\frac{H}{E\phi}\right) = 0.055 \log (8.4a/c) \quad (6)$$

from the data of Dawihl and Altmeyer [15]. Niihara *et al.* [3] found Formula B (Table I) with the restricting condition $c/a \geqslant 2.5$.

For $m = 0.5$, Anstis *et al.* [5], working on a wide range of ceramics and glasses, obtained Formula C. Lawn *et al.* [6] obtained Formula D.

2.2. Crack of Palmqvist type

Palmqvist [16, 17] suggested first that the average length of the cracks, l, emanating from the corners of a Vickers indent (Fig. 1b) might be a measure of the relative toughness at low loads. Niihara *et al.* [3] distinguished Palmqvist cracks from median cracks by using different ratios of c/a or l/a ($=(c/a) - 1$). They found that at higher values of crack-to-indent ratio ($c/a \geqslant 2.5$) the crack profile is of median type, and that at lower ratio values of the ratio ($l/a \leqslant 2.5$ or $c/a \leqslant 3.5$) the crack profile is of Palmqvist type.

Exner [18], working on low-binder content cermets, defined a crack resistance ω, based on the observed linear relationship between the indentation load and the average crack length l:

$$\omega = P/4l \quad (7)$$

Ogilvy *et al.* [19] and Perrott [20] suggested that for high-binder content WC–Co material Equation 7 should be modified to

$$\omega = (P - P_0)/4l \quad (8)$$

where P_0 is a threshold indentation load for cracking.

More recently, Niihara [21] and Warren and Matzke [22] have independently suggested a relationship of the form

$$K_{IC} = \beta_1 (H\omega)^{1/2} \quad (9)$$

where β_1 is a non-dimensional constant which depends, in Niihara's model, on the ratio of Young's modulus and hardness [21].

Shetty *et al.* [7] used Equations 8 and 3 to obtain

$$C = l + a = \frac{P - P_0}{4\omega} + \left(\frac{P}{2H}\right)^{1/2} \quad \text{for } P > P_0 \quad (10)$$

They discovered that two models (Equation 1 and Equation 10) give surprisingly very close results in their experiments for Palmqvist cracks, but they said that the Palmqvist model (Equation 10) gave a

TABLE I Available formulae*

No.	Author	Equation for K_{IC} (MPa m$^{1/2}$)	
		Median crack	Palmqvist crack
A	Niihara *et al.* [4]	$0.203(Ha^{1/2})(c/a)^{-1.5}/\phi$	–
B	Niihara *et al.* [3]	$0.129(Ha^{1/2})(E\phi/H)^{0.4}(c/a)^{-1.5}/\phi$	–
C	Anstis *et al.* [5]	$0.016(E/H)^{0.5}(P/c^{3/2})$	–
D	Lawn *et al.* [6]	$0.028(Ha^{1/2})(E/H)^{0.5}(c/a)^{-1.5}$	–
E	Shettey *et al.* [7]	–	$(HP/41)^{1/2}/[3(1 - v^2)(2^{1/2})\pi \tan \psi)^{1/3}]$
F	Niihara *et al.* [3]	–	$0.035(Ha^{1/2})(E\varnothing/H)^{0.4}(l/a)^{-0.5}/\varnothing$
G	Lankford [8]	$0.142(Ha^{1/2})(E\phi/H)^{0.4}(c/a)^{-1.56}/\phi$	
H	Laugier [9]	$0.010(E/H)^{2/3}P/C^{3/2}$	–
I	Laugier [10]	–	$0.015(l/a)^{-1/2}(E/H)^{2/3}P/C^{3/2}$

*E is the elastic modulus; H is the Vickers hardness; ϕ is a constraint factor (≈ 3); ψ is the half apex angle of the Vickers indenter ($= 68°$); P is the applied loads on indentor; v is Poisson's ratio; a, c and l are as shown in Fig. 1.

better fit overall than the half-penny crack model (Equation 1).

Shetty *et al.* [7] considered Palmqvist cracks as a two-dimensional problem and they suggested that Palmqvist cracks in equilibrium with the post-indentation crack opening due to the residual plastic zone are equivalent to a through-crack in equilibrium with a wedge of height $2h$. For the later case, Barenblatt [23] and Tweed [24] gave

$$K_{IC} = \frac{Eh}{(1 - \nu^2)(2\pi\varrho)^{1/2}} \quad (11)$$

Shetty *et al.* [7] suggested that the wedge thickness was given by the radial (plastic) expansion of the plastic zone beneath the hardness impression required to accommodate the hardness impression volume:

$$2h = 2\delta b = \frac{2^{1/2}a^3}{3\pi b^2 \tan\psi} \quad (12)$$

where ψ ($= 68°$) is the half-apex angle of the Vickers indenter, b is the plastic radius and δb is the variation of the plastic radius due to the expansion. The ratio b/a can be given by [6]

$$\frac{b}{a} = \left(\frac{E}{H}\right)^{1/2} \frac{1}{(2^{1/2}\pi \tan\psi)^{1/3}} \quad (13)$$

Thus, Shetty *et al.* [7] obtained Formula E in Table I. Formula E is just like Equation 9. Combining with Equation 3, Equation 9 or Formula E can be written as

$$\frac{K_{IC}\phi}{Ha^{1/2}} = \beta_2 (l/a)^{-1/2} \quad (14)$$

where

$$\beta_2 = \frac{1}{2^{1/2}(1 - \nu^2)(2^{1/2}\pi \tan\psi)^{1/3}}$$

Niihara *et al.* [3] discovered that there is no exact coincidence of the fracture data ($K_{IC}\phi/Ha^{1/2}$) at low values of the ratio l/a for different materials. According to the approach of Evans and Charles [1], a normalizing parameter, $(H/E\phi)^{0.4}$, is added to Equation 14 and the Formula F (Table I) can be obtained.

2.3. Mixed type of median–Palmqvist crack

Lankford [8] has disputed the analysis in the literature [3, 15] and argued that Palmqvist cracks behave in a manner identical to fully developed radial/median cracks. He noted that the ZnSe and ZnS data obtained by Evans and Charles [1] were plotted by Niihara *et al.* [3] in terms of l/a rather than c/a in spite of no evidence that ZnSe and ZnS cracks are of Palmqvist type. He replotted these data in their original form, i.e. in terms of c/a, and recombined with the other Evans and Charles data (in c/a) and with the results of Niihara *et al.* [3] (in l/a). He found that all of the Evans and Charles data are adequately described by Formula B (Table I) and it is not necessary to use Formula F to take into account the case of ZnSe and ZnS. Lankford used materials for which indentation at the lower loads produced only Palmqvist cracks with a transition to well-developed halfpenny cracks at higher loads. He modified Formula B to give Formula G. This last formula can be used in both cases: Palmqvist cracks and median cracks.

Up to now, the relationship between the Palmqvist type and median type has not been established. Lankford [8] admitted that there were still errors of about 35% in his formula for four materials. This paper attempts to find out the relationship between the two crack profiles and to find out the transformation procedure for crack profiles.

3. Experimental procedure

3.1. Materials

Zirconia-toughened alumina composites with different compositions (0 to 100% ZrO_2) were used to provide materials with a wide range of elastic and fracture properties for our study (Table II). These composites were produced by attrition milling, cold isostatic pressing and hot pressing (H.P.) at 1500° C for 15 min/30 MPa to full density [25]. The compositions with their respective Young's moduli (E) and Poisson's ratio (ν) were obtained from the law of mixtures [26].

Specimens 4 mm by 3 mm by 20 mm were machined from sintered materials; the surfaces were carefully polished successively with 6, 1 and 0.1 μm diamond pastes. After the surface preparation, specimens were annealed (1200° C, 15 min) to remove surface compressive stresses [15, 27].

3.2. Test conditions

Fracture toughness (K_{IC}) was measured for each composition using the standard SENB technique. The specimens were notched with a low-speed diamond saw to a relative depth $a/w \approx 0.4$ and a notch radius of about 0.40 μm. They were tested in three-point

TABLE II Compositions and elastic properties of alumina–zirconia composites

Material										
	Al_2O_3	A5Z0Y	A10Z0Y	A15Z0Y	A20Z0Y	A20Z1Y	A20Z2Y	A20Z3Y	A45Z3Y	TZP
Al_2O_3 (vol %)	100	95	90	85	80	80	80	80	55	0
ZrO_2 (vol %)	0	5	10	15	20	20	20	20	45	100
Y_2O_3 (mol %)	–	–	–	–	–	1	2	3	3	3
E (GPa)	392	379	370	340	250	350	349	345	296	198
ν	0.27	0.27	0.27	0.27	0.275	0.275	0.275	0.275	0.28	0.29

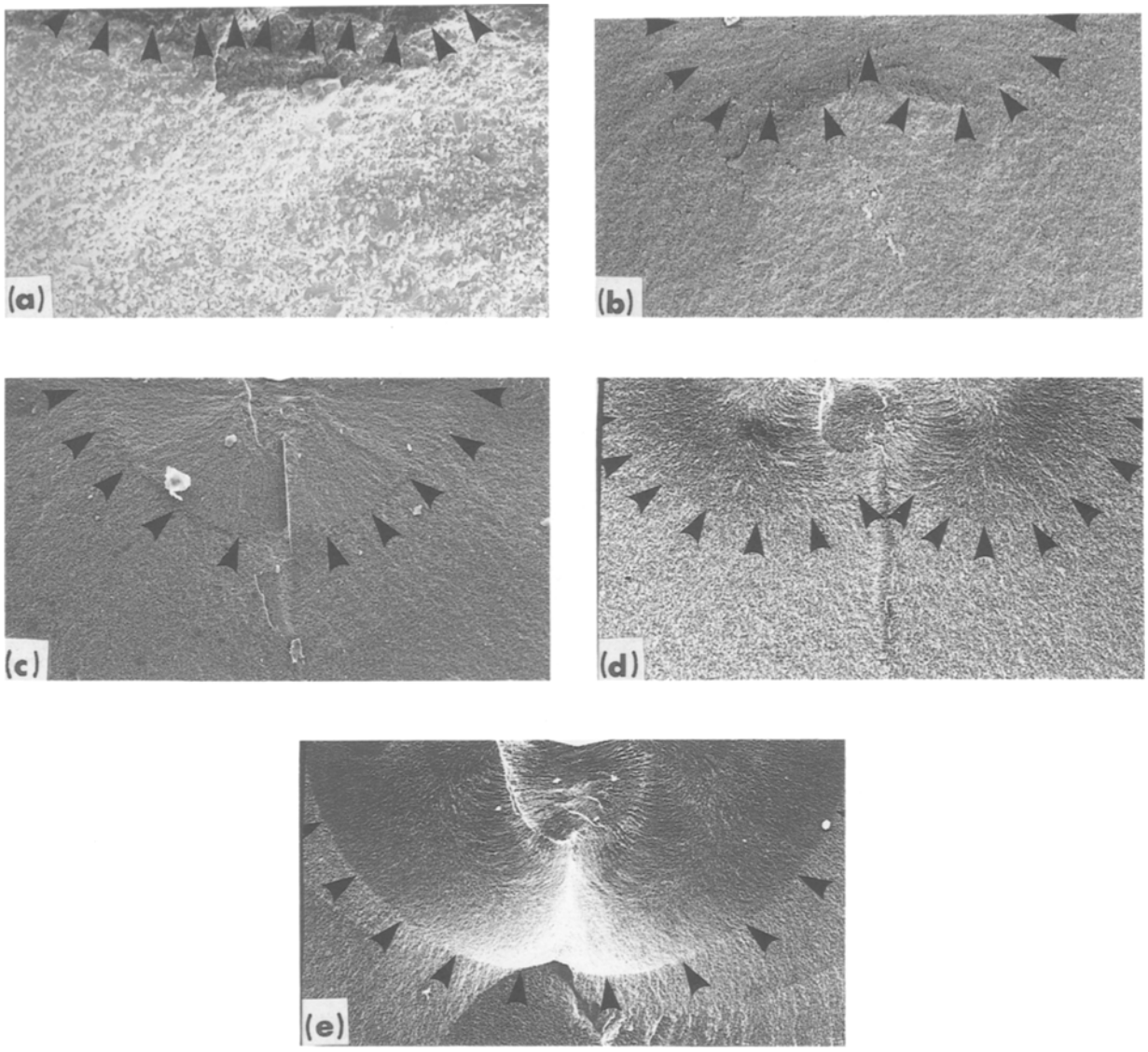

Figure 2 Crack profiles on different materials: (a) A15Z0Y, at 10 N, Palmqvist; (b) A15Z0Y, at 100 N, Palmqvist; (c) A15Z0Y, at 500 N load, median; (d) TZP, at 100 N load, Palmqvist; (e) TZP, at 500 N load, median.

bending (span = 15 mm) using a displacement rate of 0.1 mm min^{-1}, at room temperature [26].

Indentation tests were performed by the direct crack measurement (DCM) technique. The specimens were indented on the polished surface with a Vickers microhardness tester using loads ranging from 1 to 50 N and with a Vickers hardness tester using loads from 100 to 500 N. The values of c and a were measured by an optical microscope.

After indentation, the cracks induced around the indentation zone were revealed by a dye penetrant. Specimens were then broken from the indented points under bending so as to observe the crack profiles by microscope examination of the distribution of the dye penetrant inside the samples.

4. Results and discussion

4.1. Crack profiles

Figure 2 shows crack profiles (arrows indicate the edge of the crack front in each figure). In each tested material the crack profile is always of Palmqvist type (Figs 2a, b, d) when the applied load is small. When the load increases, the crack profile is modified from Palmqvist type to median type (Figs 2c, e) and the ratio d/c increases from 0.2 to 1 (d is the depth of the profile), i.e. there is a transition step from the Palmqvist type to median type (the ratio d/c is a function of the applied load). At the same load, the materials studied exhibit different crack profiles. For example, with 100 N load, the pure Al_2O_3 specimens have a crack profile of median type, whereas the TZP specimens present a Palmqvist type. When the fracture toughness values are low, it seems that the crack profile is mainly of median type: if the fracture toughness values are high enough, the crack profile is of Palmqvist type, but the transition is a function of the applied load.

Sullivan and Lauzon [28] used 296 N loads on alumina and two types of zirconia (stabilized by 4.4 and 2% Y_2O_3, respectively); they observed that the alumina material has a median type profile ($d/c = 1$), whereas the others have a Palmqvist type but with different d/c ratio. We observed that the crack profile changes from Palmqvist type to median type more easily when the material is more brittle (low toughness). Hence, the crack profile is a function of both

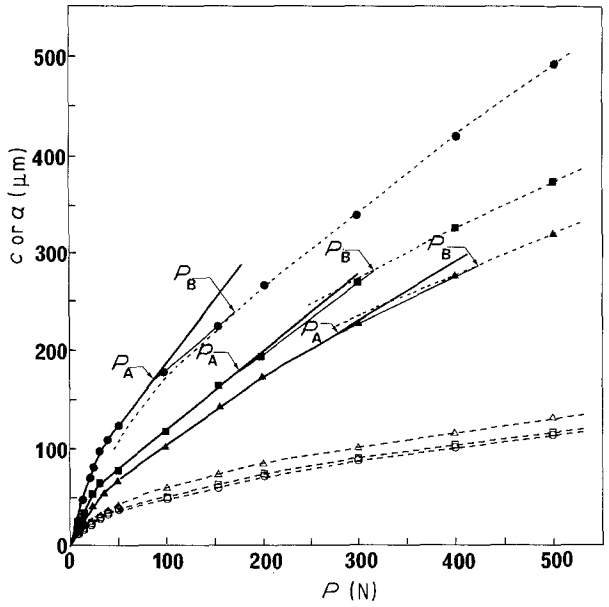

Figure 3 Variation of crack radius and impression radius with applied load P. Al_2O_3: (●) c, (○) a. A20Z3Y: (■) c, (□) a. TZP: (▲) c, (△) a. (– – –) Median crack model, (——) Palmqvist crack model.

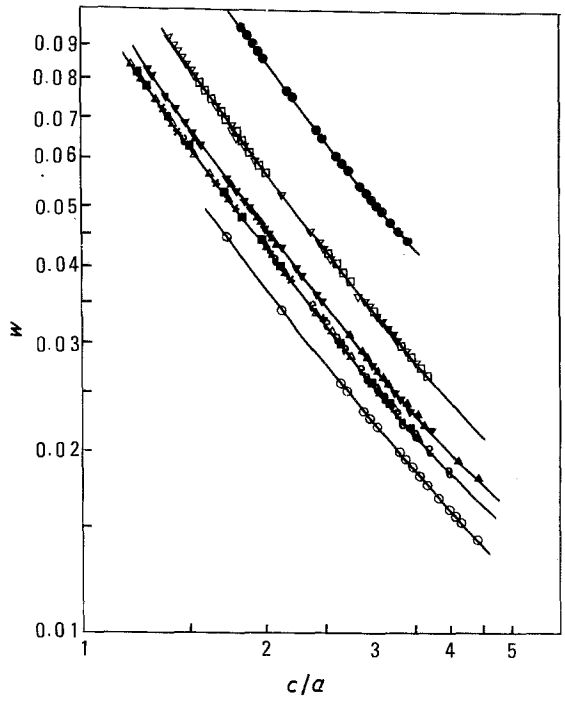

Figure 4 Variation of $W = (K_{IC}\phi/Ha^{1/2})\ (H/E\phi)^{0.4}$ against c/a. (○) Al_2O_3, (▲) A5Z0Y, (□) A10Z0Y, (▼) A15Z0Y, (■) A20Z0Y, (△) A20Z1Y, (×) A20Z2Y, (e) A20Z3Y, (▽) A45Z3Y, (●) TZP.

the applied load and the properties of the material. Between the Palmqvist type and median type there is a transition state; we do not observe a well-defined transition from Palmqvist crack to median crack.

4.2. Indentation load dependence of crack length

Figure 3 shows the crack length as a function of indentation load. The variation of crack length corresponds in fact to the Palmqvist model (Equation 7) when the applied load is small ($P \leqslant P_A$) and to the median model (Equation 1) when the load is great ($P \geqslant P_B$).

If we compare the three materials, it can be pointed out that P_A or P_B values are greater in the tough materials than in lower-toughness materials. This trend may indicate that the load range of the Palmqvist type is larger in the high-toughness materials than in the low-toughness ones.

It was noted, from Fig. 3 that the transformation of the crack profile from Palmqvist type to median type is quite regular: when $P_A \leqslant P < P_B$, the crack profile is in fact in a transition state. This is consistent with the microscopic examination of the crack profiles. These observations lead us to suggest that it is possible to find a universal model describing the two crack profiles.

4.3. Fracture curves

Using the expression of Evans and Charles [1] which has been accepted by Niihara *et al.* [3] and Lankford [8], curves (in log–log plot) of $(K_{IC}\phi/Ha^{1/2})\ (H/\phi E)^{0.4}$ against c/a were obtained (Fig. 4). The values of K_{IC} were measurd by SENB and the hardness was measured by indentation (Table III).

Figure 4 indicates that the variation of the slopes of the curves is continuous. This phenomenon is consistent with Fig. 3. When the c/a ratio is small, the crack model is of Palmqvist type; when the ratio is large, the crack model is of median type; at median ratio, the crack model is between these two types, i.e. the crack profile is in a transition state.

The slopes of the curves (Fig. 4) are not always equal to $-3/2$, but are remarkably similar for all curves at the same value of c/a: the slopes of these curves are a function of c/a for all materials which we have studied and can be fitted with a parameter equal to $[(c/18a) - 1.51]$ (value close to $-3/2$). It indicates that it is possible to describe all fracture curves in terms of c/a and that it is not necessary to use to l/a ratio to describe fraction data. This consequence is in agreement with the results of Lankford [8].

Figure 4 shows another important phenomenon: the fracture data corresponding to the different materials studies define a set of parallel curves: the slopes of all curves are defined by a parameter which is a function of the ratio c/a. Using these slopes (as a function of c/a), we can plot the fracture data of the literature from Niihara *et al.* [3]. Figure 5 compares

TABLE III Fracture toughness and Vickers hardness of alumina–zirconia composites

	Al_2O_3	A5Z0Y	A10Z0Y	A20Z0Y	A20Z1Y	A20Z1Y	A20Z2Y	A20Z3Y	A45Z3Y	TZP
K_{IC} (MPa $m^{1/2}$) ± 0.2	5.0	8.1	9.3	6.5	6.0	8.2	10.1	8.9	10.7	11.5
H_v (GPa) ± 0.3	19.4	18.9	18.4	17.9	14.0	17.7	18.5	18.4	17.0	14.4

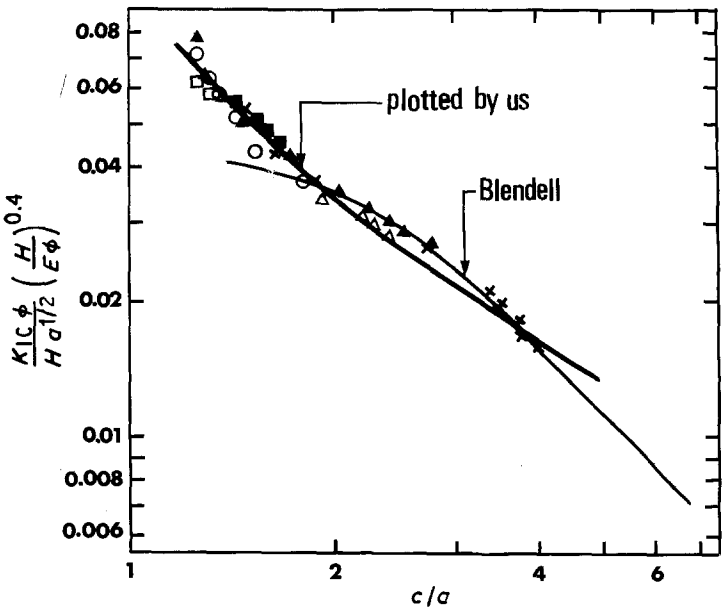

Figure 5 Comparison of normalized indentation fracture toughness data of (○) hot-pressed silicon nitride, (×) soda–lime–silica glass [3] and WC–Co alloys [15] ((▲, △) 6% Co, (■) 11% Co, (□) 15% Co) with equation curve-fitted by Blendell [14] and with another curve whose slope is $[(c/18a) - 1.51)]$ from the data of Niihara [3].

the two curves: one is plotted by Blendell [14] and the other is plotted by us. It can be noted that our curve, whose slope is a function of c/a, is consistent with the fracture data obtained by Niihara *et al.* [3] and by Dawihl and Altmeyer [15].

4.4. Poisson's ratio dependence of fracture data

Evans and Charles [1] proposed the expression

$$\frac{K_C\phi}{Ha^{1/2}} = F_1(c/a)F_2(v, \mu, b/a) \quad (15)$$

where v is Poisson's ratio, μ is the friction coefficient between the indenter and the material and b is the plastic zone radius. This equation indicates that fracture data are a function of the Poisson's ratio of the material. Shetty *et al.* [7] obtained Formula E (Table I) containing v.

Figure 4 shows that there is not an exact coincidence of the fracture data, $(K_{IC}\phi/Ha^{1/2})\,(H/E\phi)^{0.4}$, for the different materials studied. At a constant c/a ratio, the value of fracture data for TZP material is the highest and the value for alumina is the lowest. Table II shows that the value of Poisson's ratio (v) for TZP is the greatest and the value for alumina is the lowest. Figure 4 shows that there are similar W values for A20Z0Y, A20Z1Y, A20Z2Y and A20Z3Y which present the same values of Poisson's ratio and different values of fracture toughness. Therefore, the position of a curve seems to be closely related to Poisson's ratio.

As a consequence of these observations, we assume that we can separate Equation 15 as follows:

$$K_{IC}\phi/Ha^{1/2} = F_1(c/a)F_2(m, b/a)F_3(v) \quad (16)$$

with

$$F_1(c/a) = (c/a)^{(c/18a)-1.51} \quad (17)$$

$$F_2(\mu, b/a) = F_2(H/E\phi) = (E\phi/H)^{0.4} \quad (18)$$

and $F_3(v)$ is an empirically determined function. By a numerical analysis, we obtain

$$F_3(v) = \frac{1}{14\{1 - 8[(4v - 0.5)/(1 + v)]^4\}} \quad (19)$$

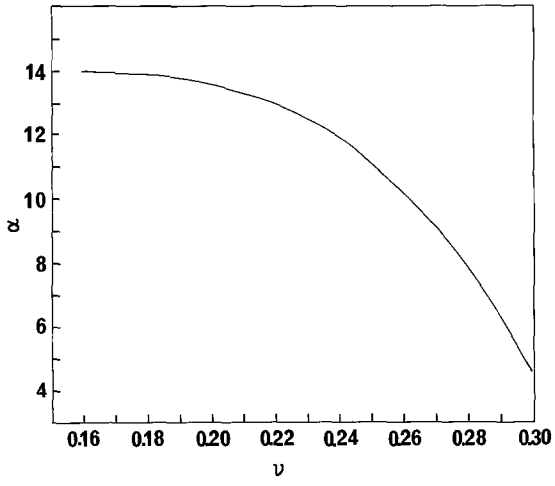

Figure 6 Variation of α against Poisson's ratio.

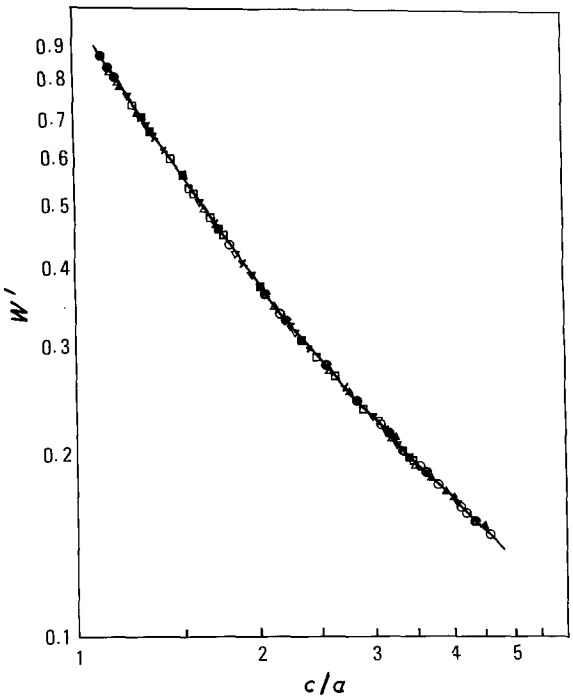

Figure 7 Variatrion of $W' = W\alpha$ against c/a. (○) Al_2O_3, (▲) A5Z0Y, (□) A10Z0Y, (▼) A15Z0Y, (■) A20Z0Y, (△) A20Z1Y, (×) A20Z2Y, (e) A20Z3Y, (▽) A45Z3Y, ● TZP.

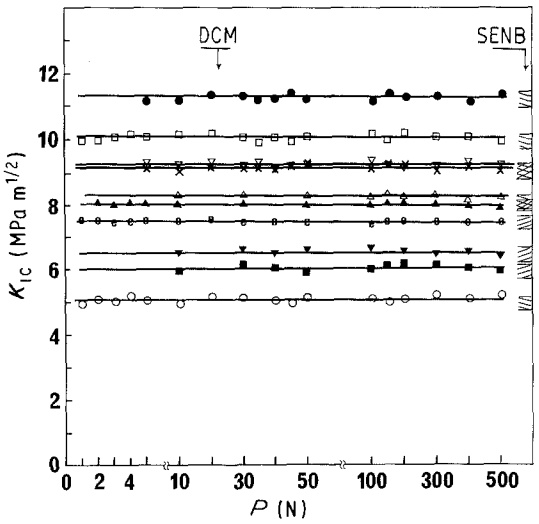

Figure 8 Comparison of fracture toughness values of Al_2O_3–ZrO_2 using Equation 21 with that measured by SENB. (○) Al_2O_3, (▲) A5Z0Y, (□) A10Z0Y, (▼) A15Z0Y, (■) A20Z0Y, (△) A20Z1Y, (×) A20Z2Y, (e) A20Z3Y, (△) A45Z3Y, (●) TZP.

We use α instead of $1/F_3(v)$ for simplifying Equation 19, where

$$\alpha = 14\left[1 - 8\left(\frac{4v - 0.5}{1 + v}\right)^4\right] \quad (20)$$

α is a non-dimensional constant and is a function of the Poisson's ratio of the material (Fig. 6): α decreases with increasing v with a corresponding increase in K_{IC}.

In Fig. 7, the different points of Fig. 4 are plotted on the same curve by including the parameter α. Now all the data shown in Fig. 7 can be expressed by

$$\left(\frac{K_{IC}\phi}{Ha^{1/2}}\right)\left(\frac{H}{E\phi}\right)^{0.4}\alpha = \left(\frac{c}{a}\right)^{(c/18a)-1.51} \quad (21)$$

4.5. Application of the new formula

Figure 8 shows that the new values of K_{IC} calculated by Equation 21 for all the loads used are just the same as those measured by SENB for the different alumina–zirconia materials.

In order to confirm this new formula (Equation 21), we have tested sintered SiC and pure alumina of different grain sizes. With different applied loads, the values of K_{IC} calculated by Equation 21 are very close to the values measured by SENB (Figs 9 and 10).

5. Conclusions

1. The crack profile induced by indentation depends on the applied load and on the properties of the material. Between the Palmqvist type and median type, a transition state is observed with a mixture of both Palmqvist and median fracture modes.

2. A new formula has been developed in order to obtain independent values of K_{IC} for brittle materials by treatment of K_{IC} values as a function of v as well as H and E.

3. With the new formula, any load can be used in an indentation test whatever the induced crack profile (Palmqvist, median or transition mode).

4. We believe that this formula could be more universal than previous ones, and hence the use of this indentation method to determine the mechanical behaviour and fracture toughness values of ceramic materials can yield intrinsic values for the material.

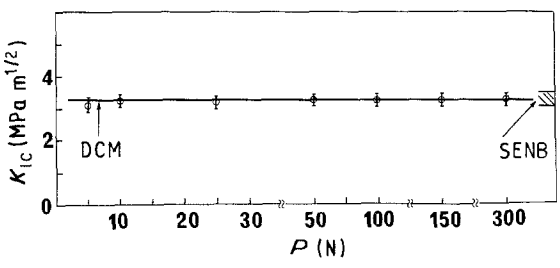

Figure 9 Comparison of fracture toughness values of SiC calculated by DCM using Equation 21 with that determined by SENB.

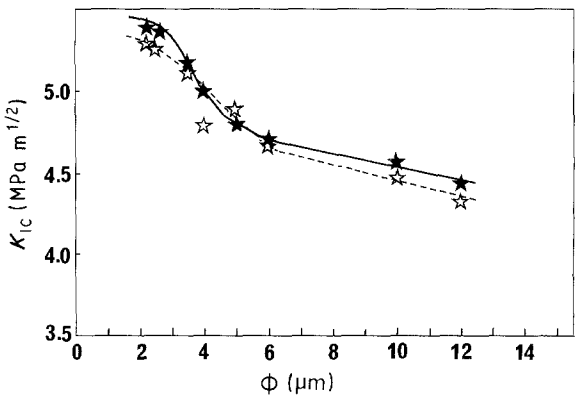

Figure 10 Comparison of fracture toughness values of pure alumina of different grain sizes calculated by (★) DCM using Equation 21 with that determined by (☆) SENB.

Acknowledgement

The authors wish to thank Dr M. T. Laugier (Materials Research Centre, NIHE, Limerick, Ireland) for discussions.

References

1. A. G. EVANS and E. A. CHARLES, *J. Amer. Ceram. Soc*, **59** (1976) 371.
2. P. MIRANZO and J. S. MOYA, *Ceram. Internat.* **10** (4) (1984) 147.
3. K. NIIHARA, R. MORENA and D. P. H. HASSELMAN, in "Fracture Mechanics of Ceramics", Vol. 5, edited by R. C. Bradt, A. G. Evans, P. P. Hasselman and F. F. Lange, (Plenum, New York, 1983) pp. 97–105.
4. K. NIIHARA, A. NAKAHIRA and T. HIRAI, *J. Amer. Ceram. Soc.* **67** (1984) C-13.
5. G. R. ANSTIS, P. CHANTIKUL, B. R. LAWN and D. B. MARSHALL, *ibid.* **64** (1981) 533.
6. B. R. LAWN, A. G. EVANS and D. B. MARSHALL, *ibid.* **63** (1980) 574.
7. D. K. SHETTY, I. G. WRIGHT, P. N. MINCER and A. H. CLAUER, *J. Mater. Sci.* **20** (1985) 1873.
8. J. LANKFORD, *J. Mater. Sci. Lett.* **1** (1982) 493.
9. M. T. LAUGIER, *ibid.* **4** (1985) 1539.
10. *Idem, ibid.* **6** (1987) 355.
11. B. R. LAWN and T. R. WILSHAW, *J. Mater. Sci.* **10** (1975) 1049.
12. B. R. LAWN and E. R. FULLER, *ibid.* **10** (1975) 2016.
13. D. B. MARSHALL and B. R. LAWN, *ibid.* **14** (1979) 2001.
14. J. E. BLENDELL, PhD thesis, M. I. T. (1979).
15. V. W. DAWIHL and G. ALTMEYER, *Z. Metallkdle* **55** (1964) 231.
16. S. PALMQVIST, *Arch. Eisenhutt.* **33** (1962) 629.
17. *Idem, Jernkontorets Ann.* **167** (1963) 208.

18. H. E. EXNER, *Trans. AIME* **245** (1969) 677.
19. I. M. OGILVY, C. M. PERROTT and J. W. SUITER, *Wear* **43** (1977) 239.
20. C. M. PERROTT, *ibid.* **47** (1978) 81.
21. K. NIIHARA, *J. Mater. Sci. Lett.* **2** (1983) 221.
22. R. WARREN and H. MATZKE, in Proceedings of International Conference on The Science of Hard Materials, Jackson, Wyoming, August 1981, edited by R. K. Viswanadham, D. J. Rowcliffe and J. Gurland (Plenum, New York, 1983) p. 563.
23. G. I. BARENBLATT, *Adv. Appl. Mech.* **7** (1962) 56.
24. J. TWEED, *J. Elasticity* **1** (1971) 29.
25. A. LERICHE, G. MOORTGAT, F. CAMBIER, P. HOMERIN, G. ORANGE, F. THEVENOT, G. FANTOZZI, in "Zirconia 86", to be published in "Advances in Ceramics", Vol. 24, (American Ceramic Society).
26. G. ORANGE and G. FANTOZZI, *Matér. Téchn.* **3** (1988) 29.
27. Y. ILUMA and A. V. VIRKAR, *J. Mater. Sci.* **19** (1984) 2233.
28. J. D. SULLIVAN and P. H. LAUZON, *J. Mater. Sci. Lett.* **5** (1986) 247.

Received 25 July 1988
and accepted 14 April 1989